

**NIGHTTIME CONVECTION, TEMPERATURE INVERSIONS, AND DIURNAL VARIATIONS AT LOW ALTITUDES IN THE MARTIAN TROPICS.** D. P. Hinson<sup>1,2</sup>, R. M. Haberle<sup>3</sup>, A. Spiga<sup>4</sup>, S. Tellmann<sup>5</sup>, M. Pätzold<sup>5</sup>, S. W. Asmar<sup>6</sup>, and B. Häusler<sup>7</sup>. <sup>1</sup>Carl Sagan Center, SETI Institute, Mountain View, CA, USA (dhinson@seti.org); <sup>2</sup>Dept. of Electrical Engineering, Stanford University, Stanford, CA, USA; <sup>3</sup>NASA/Ames Research Center, Mountain View, CA, USA; <sup>4</sup>Université Pierre et Marie Curie, Paris, France; <sup>5</sup>Universität zu Köln, Cologne, Germany; <sup>6</sup>Jet Propulsion Laboratory, Pasadena, CA, USA; <sup>7</sup>Universität der Bundeswehr München, Neubiberg, Germany.

**Introduction:** We are using radio occultation (RO) measurements from Mars Express (MEX), Mars Reconnaissance Orbiter (MRO), and Mars Global Surveyor (MGS) to characterize the atmospheric structure and diurnal variations in the lowest few scale heights of the tropics. We focus on northern spring and summer, using observations from 4 martian years at local times of 4-5 and 15-17 h.

We supplement the observations with results obtained from the NASA/Ames Mars General Circulation Model (MGCM) [1] and from large-eddy simulations with the Martian Mesoscale Model of the Laboratoire de Météorologie Dynamique [2]. The RO measurements provide new constraints for validation of the models, while the models provide a foundation for interpreting the observations.

**Results:** We previously investigated the depth of the daytime convective boundary layer (CBL) and its variations with surface elevation and surface properties [3, 4, 5]. Figure 1 shows the temperature structure in late afternoon RO profiles from two locations. The depth of the mixed layer varies markedly with surface elevation, so that the peak height of the daytime CBL differs by 8 km between these two regions.

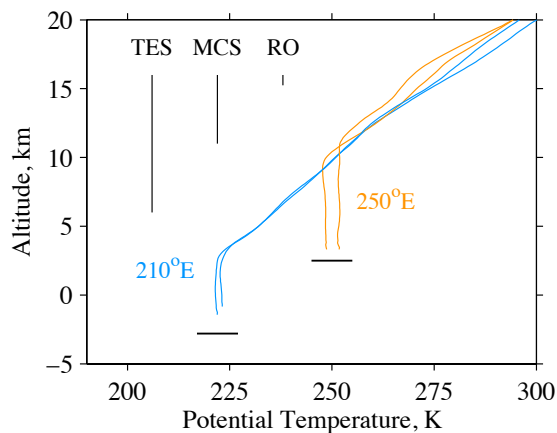


Figure 1: MEX RO profiles in northern spring ( $L_s = 25^\circ$ ). Orange lines show profiles from the Tharsis region ( $250^\circ\text{E}$ ,  $20\text{-}25^\circ\text{N}$ ). Blue lines show profiles from Amazonis ( $210^\circ\text{E}$ ,  $20\text{-}25^\circ\text{N}$ ). The local time is 15.6 h. Each profile contains a CBL, where the potential temperature is nearly constant.

Figure 1 also compares the vertical resolution of temperature profiles retrieved by the MGS Thermal Emission Spectrometer (TES), the MRO Mars Climate Sounder (MCS), and the radio occultation (RO) technique. The vertical resolution of the RO profiles yields unique insight into the structure of the lower atmosphere.

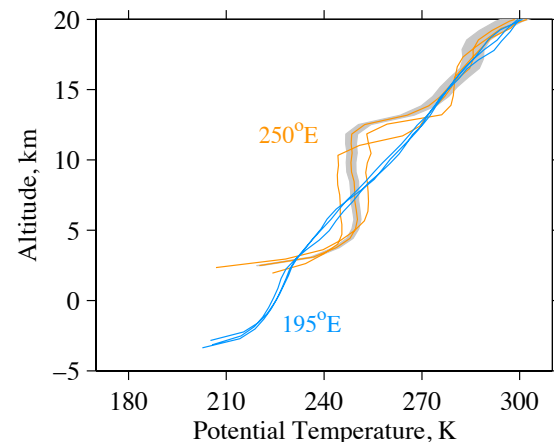


Figure 2: MGS RO profiles in northern summer ( $L_s = 140^\circ$ ). Orange lines show profiles from the Tharsis region ( $250^\circ\text{E}$ ,  $20\text{-}25^\circ\text{N}$ ). Blue lines show 3 profiles from contemporaneous measurements in Amazonis ( $195^\circ\text{E}$ ,  $20\text{-}25^\circ\text{N}$ ). The local time is 4.2 h. A detached mixed layer, where the potential temperature is constant, appears above Tharsis but not in Amazonis. The shaded region corresponds to the 1-sigma uncertainty.

We are also examining unusual aspects of the temperature structure observed at night [6], which provide additional constraints on the diurnal cycle in the tropics. Figure 2 shows examples of the RO measurements from the same two regions as in Figure 1. Most important, predawn profiles above Tharsis contain an unexpected layer of neutral static stability at pressures of 200-300 Pa with a depth of 4-5 km. Nighttime profiles in Amazonis show no sign of a detached mixed layer.

The pre-dawn mixed layer above Tharsis is capped by a 10-K temperature inversion (not shown), which may arise in response to radiative cooling from a water ice cloud layer [7]. What's new about the observations in Figure 2 is the further implication that cloud-

induced radiative cooling can generate convective instability below the inversion.

We have performed a pair of simulations with the NASA/Ames MGCM to explore this hypothesis. The results confirm that nighttime radiative cooling by a water ice cloud can produce a predawn mixed layer capped by a temperature inversion – the simulated temperature structure closely resembles the Tharsis profiles in Figure 2. Neither the predawn mixed layer nor the overlying inversion appears in a “passive” baseline simulation that omits the effects of cloud radiation.

**Discussion:** These regional variations in the nighttime temperature structure appear to arise in part from large-scale variations in topography, which have several notable effects. First, the CBL is much deeper in the Tharsis region than in Amazonis, owing to a roughly 6-km difference in surface elevation [3, 5]. Second, large-eddy simulations show that daytime convection is not only deeper above Tharsis but also considerably more intense than it is in Amazonis [4]. Finally, the daytime surface temperatures are comparable in the two regions, so that Tharsis acts as an elevated heat source throughout the CBL. These topographic effects are expected to enhance the vertical mixing of water vapor above elevated terrain, which might lead to the formation and regional confinement of nighttime clouds.

We are surveying the RO profiles from MGS and MRO to further characterize the spatial distribution of the predawn mixed layers and their seasonal evolution. We also plan to compare the RO results with nighttime observations of water ice clouds [8, 9, 10]. Our interpretation of the results will rely heavily on MGCM simulations.

**Acknowledgments:** This research is funded in part by Grant NNX12AL48G of the Mars Data Analysis Program and by NASA support for the U.S. Investigators of the European Mars Express Mission.

**References:** [1] Haberle R. M. et al. (2011) *4<sup>th</sup> International Workshop on the Mars Atmosphere: Modelling and Observation*. [2] Spiga A. and F. Forget (2009) *JGR*, 114(E2), E02009. [3] Hinson D. P. et al. (2008) *Icarus*, 198, 57–66. [4] Spiga A. et al. (2010) *Q. J. R. Meteorol. Soc.*, 136, 414–428. [5] Tellmann S. et al. (2013) *JGR*, 118, 306–320. [6] Hinson D. P. et al. (2014) *Icarus*, submitted. [7] Haberle R. M. et al. (1999) *JGR*, 104, 8957–8974. [8] Wilson R. J. et al. (2007) *GRL*, 34, L02710. [9] McCleese D. J. et al. (2010) *JGR*, 115(E12), 12016. [10] Heavens N. G. et al. (2010) *GRL*, 37, L18202.